Global Change Biology

WILEY

Global Change Biology

RESEARCH ARTICLE OPEN ACCESS

Wildfire-Induced Losses of Soil Particulate and Mineral-Associated Organic Carbon Persist for Over 4 Years in a Chaparral Ecosystem

Alexander H. Krichels[1,2] | Elizah Z. Stephens[2] | Chloe Reid[2] | M. Fabiola Pulido Barriga[3] | Maria E. Ordoñez[3] | Jennie R. McLaren[4] | Meg Kargul[5] | Loralee Larios[5] | Sydney I. Glassman[3] | Peter M. Homyak[2]

[1]USDA Forest Service Rocky Mountain Research Station, Albuquerque, New Mexico, USA | [2]Department of Environmental Sciences, University of California, Riverside, California, USA | [3]Department of Microbiology and Plant Pathology, University of California, Riverside, California, USA | [4]Department of Biological Sciences, University of Texas at El Paso, El Paso, Texas, USA | [5]Department of Botany and Plant Sciences, University of California, Riverside, California, USA

Correspondence: Alexander H. Krichels (alexander.krichels@usda.gov)

Received: 9 January 2025 | **Revised:** 17 July 2025 | **Accepted:** 22 July 2025

Funding: This work was supported by the Division of Environmental Biology (1916622), United States Department of Agriculture National Institute of Food and Agriculture (2022-67014-36675), and Department of Energy Biological and Environmental Research (DE-SC0023127).

Keywords: ^{13}C | bacteria | extracellular enzymes | fungi | MAOM | POM | pyrogenic organic matter | soil carbon

ABSTRACT

Wildfires can lower soil carbon (C) stocks directly through combustion, but also indirectly during post-fire recovery if microbial C demands outpace photosynthetic C inputs. However, how much C is respired by soil microorganisms post-fire may depend on wildfire effects on particulate organic carbon (POC; mostly plant material accessible to microbes) and/or mineral-associated organic carbon (MAOC; considered C protected by minerals from decomposers), meaning assessment of wildfire impacts on these pools is necessary to predict microbial decomposition rates and, thus, the fate of soil C. Here, we measured POC, MAOC, pyrogenic organic matter C, plant cover, extracellular enzyme activity (EEA), and microbial community abundance and composition 17 days, and 1, 3, and 4 years after the Holy Fire burned 94 km^2 of fire-adapted chaparral. The wildfire immediately decreased POC by 50% (from 51 ± 21 to 26 ± 6 g C kg^{-1}) and MAOC by 33% (from 9.3 ± 0.9 to 6.3 ± 0.9 g C kg^{-1}), consistent with MAOC being less vulnerable to loss than POC. POC decreased by another 38% 1 year post-fire, consistent with increases in microbial abundance and EEA suggesting increased microbial decomposition. Between 1 and 4 years after the fire, cover of the dominant shrub (*Arctostaphylos glandulosa*) increased from $3.9\% \pm 1.6\%$ to $16\% \pm 5.4\%$ (compared to $58\% \pm 4.6\%$ in unburned plots), marking the end of net soil C losses. Still, soil C did not increase between 1 and 4 years post-fire, suggesting plant C inputs did not outpace microbial respiration, a finding consistent with isotopically heavier C from microorganisms raising bulk soil $\delta^{13}C$ values. As global changes favor increases in wildfire frequency and severity, C losses via combustion and decomposition may outpace plant C inputs during the first 4 years post-fire in chaparral, slowing the replenishment of soil C stocks.

1 | Introduction

Wildfires are projected to continue increasing in frequency and severity with global climate change, with implications for the storage of carbon (C) in soils (Abatzoglou et al. 2019; Pellegrini, Harden, et al. 2021; Riley and Loehman 2016). Soil C can be immediately depleted if wildfires combust soil organic matter (SOM; Walker et al. 2019; Wardle et al. 2003) and can continue to decrease in the years following fire if photosynthetic C inputs are outpaced by heterotrophic respiration (Pellegrini, Harden,

et al. 2021). How soil C stocks change in response to wildfires with time may, therefore, depend on whether SOM is accessible to microbial decomposers in particulate form (i.e., particulate organic carbon; POC) or if it is bound to minerals that protect C from decomposition (i.e., mineral-associated organic carbon; MAOC; Cotrufo et al. 2019; Lavallee et al. 2020; Wang et al. 2023). Furthermore, wildfires can leave behind pyrolyzed organic matter (PyOM) that may be more chemically complex and difficult for microbes to decompose (DeLuca et al. 2020; Hatten et al. 2008). Yet, the relative effects of wildfires on plant C inputs, microbial C decomposition, C volatilization, and the bioavailability of C remaining in the soil post-fire are currently understudied, especially in shrubland ecosystems that make up ~13% of the world's land area (Maestre et al. 2021). Understanding controls over the loss and accumulation of soil C in burned landscapes is necessary to predict changes to and manage ecosystem C stocks as fire return intervals are predicted to shorten with global climate change.

Wildfires can combust much of the C in aboveground biomass, but they do not always combust C stored in SOM (Pellegrini et al. 2023). Combustion of SOM has primarily been documented in forested ecosystems, where burning of large trees and organic materials can generate enough heat to burn surface soils (Ansley et al. 2006; DeBano 2000; Pellegrini et al. 2023; Walker et al. 2019; Wardle et al. 2003). Yet, limited access to post-fire landscapes has prevented immediate measurements of soil C cycling that are necessary to understand how burn severity affects C losses. In addition to burn severity, the susceptibility of soil C to volatilization may depend on whether C is associated with minerals that offer protection against decomposition and loss (i.e., MAOC). Recent studies suggest that MAOC may volatilize at a higher temperature than POC, potentially allowing wildfires to preferentially deplete soil POC over MAOC (Wang et al. 2023). However, it is not clear if the higher volatilization temperatures of MAOC translate to greater protection of C in the field (Pellegrini, Caprio, et al. 2021).

Even if wildfires may not directly combust soil C during the fire, post-fire environments may still promote soil C losses if microbial respiration outpaces photosynthetic C inputs (Pellegrini, Harden, et al. 2021). For example, photosynthetic C inputs may be limited during the 10–30 years it takes for woody vegetation to reach pre-fire abundance and density (O'Leary 1984; Vogl and Schorr 1972). While wildfires can also lower microbial abundance and alter community composition (Dooley and Treseder 2012; Dove and Hart 2017; Pérez-Valera et al. 2018; Pressler et al. 2019; Whitman et al. 2022), these changes do not necessarily slow C losses because microbial communities do not always predict respiration rates (Graham et al. 2016; Rocca et al. 2015; Schimel and Schaeffer 2012). Indeed, fast-growing pyrophilous bacteria and fungi that colonize burned soils within days to months after fire (Enright et al. 2022; Pulido-Chavez et al. 2022; Whitman et al. 2019) may be able to decompose organic matter just as well as microbial communities in unburned soils. As such, respiration rates for pyrophilous bacteria and fungi may outpace photosynthetic C inputs from recovering vegetation, depleting soil C pools in the post-fire environment. However, if burning preferentially depletes soil POC over MAOC (Wang et al. 2023), then the C that persists in post-fire environments may be protected by minerals against microbial respiration, potentially preventing further C loss after severe fires (Cotrufo et al. 2019; Lavallee et al. 2020; Rocci et al. 2021). Therefore, understanding which soil C fractions are prone to persist after wildfires and when microbes may begin to meet their C demands from new photosynthetic C inputs is key to predicting the trajectory of soil C stocks after wildfires.

In addition to releasing soil C to the atmosphere during respiration, soil microorganisms also play key roles in building soil C pools. Microorganisms produce extracellular enzymes that break down plant litter into labile soil C that comprises POC, while also assimilating and transforming labile C into microbial residues that are major components of MAOC (Liang et al. 2017; Lavallee et al. 2020; Camenzind et al. 2023). Fungi may be especially important in breaking down plant litter into labile soil C because they produce oxidative extracellular enzymes that decompose lignin-rich wood and chemically complex PyOM (Floudas et al. 2012; Huang et al. 2022; Nelson et al. 2024; Riley et al. 2014). Furthermore, mycorrhizal fungi provide nutrients to plant roots, aiding the recovery of vegetation after wildfires and helping to accelerate photosynthetic C inputs to the soil (Allen et al. 1999; Horton et al. 2011). Plants also share C with mycorrhizal fungi, favoring the production of mycelium that makes up SOM (Ekblad et al. 2013; Högberg and Högberg 2002). Because fungal and bacterial biomass are composed of isotopically heavier C than plants, soil $\delta^{13}C$ values may increase as microbial biomass contributions to soil C increase (Ehleringer et al. 2000; Werth and Kuzyakov 2010; Klink et al. 2022). As such, soil $\delta^{13}C$ values may offer insights into the fate of soil C in post-fire environments and help understand how microbial and plant succession alter soil C pools.

Here, we ask: (i) how do soil mineral associations and soil burn severity affect how much C is lost from surface soils after wildfire? And (ii) how does the recovery of plant and microbial communities affect the trajectory of surface soil C pools after wildfire? To answer these questions, we monitored soil $\delta^{13}C$, MAOC, POC, PyOM-C, bacterial and fungal abundance, potential extracellular enzyme activity, leaf litter decomposition, microbial community composition, and plant and litter cover between 17 days and 4 years after a severe wildfire was extinguished in a chaparral shrubland in southern California. We hypothesized that POC is more susceptible to volatilization, resulting in a greater loss of POC compared to MAOC immediately after burning (H1). We also hypothesized that higher soil burn severity (inferred from ash depth) would volatilize more C, resulting in progressively lower MAOC and POC pools in soils with greater burn severities (H2). Finally, we hypothesized that microbial respiration would outpace photosynthetic C inputs to the soil, decreasing POC in the months after burning, followed by an increase in soil C once plants reestablished (H3).

2 | Methods

2.1 | Site Description

This study was conducted within the Holy Fire burn scar in the Cleveland National Forest. The Holy Fire burned 94 km^2 of manzanita-dominated chaparral shrubland between August 6 and September 13, 2018. Seventeen days after the fire was

extinguished, we established nine plots (1195–1285 m elevation); six of these plots were within the burn scar of the Holy Fire (slope 33%–57%, where a 100% slope is at a 45° angle), while the other three served as control unburned plots (Figure S1; Pulido-Chavez et al. 2022). We measured ash depth as an index of fine-scale soil burn severity (Pulido-Chavez et al. 2022) because 30 m^2 BAER measurements may not coincide with microbial or plant recovery (Bahram et al. 2013); all burned plots were established in areas of "moderate" soil burn severity based on BAER classifications (Nicita and Halverson 2018). Each plot (~25 m^2) consisted of four 1 m^2 subplots located 5 m from the center of the plot in each cardinal direction (i.e., N, S, E, W; Figure S1). All nine plots had similar aspects, slopes, elevations, and pre-fire vegetation dominated by manzanita (*Arctostaphylos glandulosa*) and chamise (*Adenostoma fasciculatum*) shrubs.

The climate at the site is Mediterranean with hot, dry summers (average 3.9 ± 9.7 mm precipitation per month from June through September since 1995) and cool, wet winters (average 54.8 ± 53.4 mm precipitation per month from October through May since 1995). Annual temperature averages 17.5°C ± 0.68°C and total annual precipitation averages 403 ± 180 mm. Precipitation and temperature data are based on monthly summaries for the El Cariso weather station (RAWS USA Climate Archive 2024). Soils in all the control plots are classified as Lithic Haploxerolls and mapped in the Friant series, as are soils in half of the plots within the burn scar. Because of steep slopes, fire burn patterns, and limited accessibility to the burn scar, the remaining burned plots were established on Typic Xerorthents, mapped in the Cieneba series. Soils from both series are shallow sandy and gravelly loams (Soil Survey Staff 2024).

2.2 | Soil Sampling

At the first timepoint, we measured and averaged ash depth at 3 points within the 1 m^2 subplots as an index of fine-scale soil burn severity (Pulido-Chavez et al. 2022). We sampled soils from all four subplots within each of the nine plots starting 17 days after the fire was extinguished—before rainfall washed any ash away—and returning 371, 1092, and 1460 days later (roughly 1, 3, and 4 years post-fire). All samples were collected in the fall to minimize the effect of seasonality on soil C dynamics. Soil samples from the surface horizon (0–10 cm depth) were collected using an ethanol-sterilized bulb planter after removing the litter (unburned plots) and ash layers (burned plots) from the surface. Soils were transported back to the lab within hours of collection, where they were stored overnight at 4°C. Soils were sieved to 2 mm within 24 h of sampling. One subsample (> 5 g) was frozen at −80°C for molecular analyses, with the remaining soil left to air dry for physiochemical analyses. Soil pH was measured in a slurry of 2:1 water to dry soil using a pH meter (Thermo Scientific; Orion Versastar Pro meter equipped with ROSS Ultra pH electrode). We only measured soil C concentrations and extracellular enzyme activity from soils collected from the N and S direction subplots. While microbial communities were measured in all four subplots (Pulido-Chavez et al. 2022), we only present microbial data from samples that were also analyzed for soil C. We also collected soil cores (0–5 cm depth, 5 cm diameter) 25 days after the fire from all four subplots within each plot to measure soil bulk density. Bulk density was calculated by dividing the dry soil weight (minus any coarse fragments > 2 mm) by the volume of the soil corer.

2.3 | Soil Carbon Pools

To measure POC and MAOC, we used density fractionation to separate SOM into particulate organic matter (POM), mineral-associated organic matter (MAOM), and sand-associated organic matter from the N and S subplots of each plot at each time point. Because little C was detected in the sand fraction (mean C in sand = 2.5 g-C kg^{-1}), and MAOM plays a stronger role in stabilizing C (Poeplau et al. 2018; Püspök et al. 2022), we do not present sand-associated organic matter here. To fractionate organic matter, 5 g oven-dried soil (60°C) was mixed with 1.65 g cm^{-3} sodium polytungstate (SPT) and dispersed using 200 J mL^{-1} ultrasonic energy at 60 W. The soil solution was then centrifuged at 2500 *g* for 60 min. The floating fraction was aspirated onto a 0.45 μm glass fiber filter for vacuum filtration and rinsing with deionized (DI) water. The remaining pellet was then washed with DI water and passed through a sieve to separate sand (> 53 μm) from the silt and clay (< 53 μm) fractions. The three soil fractions from each sample were then oven-dried (60°C) for 24 h, weighed, and finely ground before being analyzed for soil C and N content on an elemental analyzer (Flash EA 1112 CN; Thermo Fisher Scientific INC.). On average, we recovered 98% ± 4.9% of soil mass, 117% ± 37% of soil N, and 95% ± 25% of soil C.

We calculated POC and MAOC on a per mass basis by multiplying the percent C by the weight of soil recovered of each fraction and dividing this by the initial amount of bulk soil. We also calculated POC and MAOC stocks by multiplying C concentration by bulk density measured 25 days after the fire and soil depth (10 cm) to estimate how much C is in these surface soils. However, fire can compact soils by breaking down organic-rich aggregates (Certini 2005; Stoof et al. 2010), potentially inflating C stocks calculated using bulk density (Fowler et al. 2023; von Haden et al. 2020). As such, presenting C on a per mass basis is likely a more accurate comparison of C availability in burned versus unburned soils.

We also measured $\delta^{13}C$ of POC and MAOC to assess if plant C inputs and microbial respiration affected soil $\delta^{13}C$. We measured $\delta^{13}C$ values from samples collected at the first (17 days, to determine a fire effect) and last (4 years, to determine if values returned to pre-fire) timepoints at the UC Riverside Facility for Isotope Ratio Mass Spectrometry (FIRMS; https://ccb.ucr.edu/facilities/firms).

To estimate the concentration of pyrolyzed organic matter (PyOM) in soils, we digested soil samples with weak nitric acid and hydrogen peroxide (Kurth et al. 2006; Licata and Sanford 2012; Pingree et al. 2012). This weak acid extraction estimates PyOM accurately in soils with 0.5%–5% charcoal, oxidizes very little non-pyrogenic C, and is more economical than nuclear magnetic resonance (Kurth et al. 2006; Maestrini and Miesel 2017). Soil samples (1 g) were oven dried (60°C) before being mixed with 10 mL of 1 M nitric acid and 20 mL of 30%

hydrogen peroxide in a 100 mL digestion tube. The solution was mixed by swirling the tube and allowed to sit at room temperature for at least 5 min. The digestion tube was then incubated at 100°C for 16 h, after which the samples were cooled before filtering (Whatman #2). The soil that remained on the filter paper was then dried before being analyzed for soil C content. Carbon in PyOM (PyOM-C) was calculated as the percent C times the mass of the digested soil sample divided by the weight of the initial undigested soil.

2.4 | Soil Potential Extracellular Enzyme Activity and Aboveground Leaf Litter Decomposition Rates

We measured the potential activity of soil extracellular hydrolytic enzymes using substrates tagged with fluorescing methylum-belliferone (MUB) or 7-amido-4-methyl-coumarin (MC) (Marx et al. 2001). The activity of the starch-degrading hydrolytic enzyme α-glucosidase (AG) was measured using 4-MUB-α-d-glucopyranoside. The activity of the cellulose-degrading hydrolytic enzyme β-glucosidase (BG) was measured using 4-MUB-β-d-glucopyranoside. The activity of the cellulose-degrading hydrolytic enzyme 1,4-β-cellobiohydrolase (CBH) was measured using 4-MUB-β-D-cellobioside. The activity of the chitin-degrading and N-acquisition hydrolytic enzyme N-acetyl-β-D-glucosaminidase (NAG) was measured using 4-MUB N-acetyl-β-D-glucosaminide. The activity of the peptide-degrading and N-acquisition hydrolytic enzyme l-Leucine aminopeptidase (LAP) was measured using L-Leucine-7-amido-4-methylcoumarin. Finally, the activity of the organic P-degrading and P acquisition hydrolytic enzyme Phosphomonoesterase (PHO) was measured using 4-MUB-phosphate.

All enzyme assays were carried out in 96-well plates consisting of 100 μL substrate and 100 μL soil slurry. Soil slurries were made by blending soil in a universal buffer solution adjusted to pH 6.5 (1:125 soil weight to volume). For each substrate, we measured the background fluorescence of soils and substrate, and the quenching of MUB by soils, and used standard curves of MUB or MC to calculate the rate of substrate hydrolyzed. Fluorescence was measured at 360 nm excitation and 460 nm emission in a plate reader (Tecan, Männedorf, Switzerland), five times over 3 h, following methods adapted from Saiya-Cork et al. (2002) and McLaren et al. (2017). We also measured the activity of the lignin-degrading enzymes phenol oxidase (Phenol) and peroxidase (Perox) using L-3,4-dihydroxyphenylalanine substrate. Color absorbance was measured at 460 nm in a plate reader after a 24-h incubation (McLaren et al. 2017).

We measured aboveground leaf litter decomposition rates using a litter mesh bag approach starting 1 year post-fire. First, we collected recently senesced leaf litter from *A. glandulosa* shrubs adjacent to our control plots. This litter was brought to the lab, where it was shredded using a blade grinder to represent degradation via macro consumers. The ground litter (3 g) was then sealed within a pouch made from nylon screening (0.5 mm mesh size) and gamma irradiated at 12,000–14,000 Gy for 2.5 days at the University of California-Irvine, Dept of Radiation Oncology, to reduce native bacteria and fungi as previously established (Glassman et al. 2018). Approximately 1 month after collecting the litter, sterile decomposition bags were placed inside a cage made of wire (1-cm mesh size) to protect the mesh bags from destruction by insects and larger animals. A total of three litter bags per plot were randomly fixed to the ground using wire stakes on December 17, 2019 (460 days since fire). The first litter bag was collected 5 months after deployment (613 days since fire), the second was collected at 13 months (860 days since fire), and the third at 2 years (1225 days since fire). In the lab, the leaf litter was removed from the litter bags, dried overnight at 65°C, and reweighed to calculate mass loss. Decomposition rates were calculated as the percent of litter mass remaining after the field incubation.

2.5 | Shrub, Herb, and Grass Cover

We measured the cover of all plants—a strong proxy for aboveground biomass (Sanaei et al. 2018)—in each of the 1-m^2 subplots at 286, 376, 612, 718, 966, and 1314 days after the fire was extinguished. We were unable to measure plant cover at the same time as soil samples were collected due to logistical constraints. We note that most plants took multiple months to resprout, limiting the usefulness of earlier vegetation sampling. Plant cover was measured by visually estimating vegetative cover for all species contained within each 1-m^2 subplot. Plant cover was allowed to go over 100% for a given subplot due to overlapping plant canopies. We then grouped plant cover based on categories (shrub, subshrub, herb, or grass) that capture successional changes in plant composition (Table S1). Because plant cover may not relate to belowground C inputs, we also assessed changes in plant C inputs by measuring soil and plant $\delta^{13}C$. We measured the $\delta^{13}C$ of leaves collected from dominant shrubs in burned and unburned plots. Within burned plots, leaves were collected from individual shrubs that had resprouted vegetatively or grown from seed. We attempted to sample six shrubs of each species from each type (adult, resprouter, or seedling), but only found five resprouted *A. fasciculatum* shrubs and three seeded *A. fasciculatum* shrubs.

2.6 | DNA Extraction, Sequencing, qPCR, and Bioinformatics

We extracted DNA from frozen (−80°C) soils to measure the abundance, alpha diversity, and beta diversity of bacteria and fungi. For the 17-day, 1-year, and 3-year samples, we extracted DNA from 0.25 g of soil (Qiagen DNeasy PowerSoil Kits, PowerSoil Pro, Hilden, Germany), with a slight modification to the manufacturer's protocol (extending centrifugation time to 1.5 min after adding C3; Pulido-Chavez et al. 2022). For the 4-year samples, DNA was extracted (Qiagen PowerSoil Pro Kits, PowerSoil Pro, Hilden, Germany) due to the discontinuation of the previously used kits. To enhance DNA recovery, we incubated the soil sample overnight (700 μL CD1 + 100 μL ATL at 4°C) before proceeding with the manufacturer's instructions. We used the primer pair 515F-806R to amplify the V4 region of the 16S rRNA gene for archaea and bacteria (Caporaso et al. 2011) and the primer pair ITS4-fun and 5.8S to amplify the

ITS2 region for fungi (Taylor et al. 2016) and sequenced at the UCR Institute for Integrative Genome Biology (Illumina MiSeq 2×300 bp) using previously published protocols (Pulido-Chavez et al. 2022).

We used qPCR to estimate bacterial and fungal abundance in our DNA extracts. The Eub338/Eub518 primers were used for bacteria (Fierer et al. 2005) and the FungiQuant-F/FungiQuant-R primers were used for fungi (Liu et al. 2012). The qPCR master mix was prepared with 1× of iTaq SYBR mix (Bio-Rad) and 0.4 μM final concentration of primers, with 1 μL of DNA and ultrapure water for a final volume of 10 μL.

Each reaction was run in triplicate in 384 well plates on a PCR system (BioRad CFX Opus 384 Real-Time PCR System) starting at 94°C for 5 min, followed by 40 cycles of a denaturing step at 94°C for 20 s, primer annealing at 52°C for bacteria or 50°C for fungi at 30 s, and an extension step at 72°C for 30 s. Standards were generated by cloning the 16S region of *Escherichia coli* with a plasmid length of 157 or the 18S region of *Saccharomyces cerevisiae* with a plasmid length of 353 into puc57 plasmid vectors (GENEWIZ Inc., NJ, USA) as previously established (Pulido-Chavez et al. 2022). Melt curves were generated and copy numbers were extracted using the following equation, Gene copy number = (Starting quantity of DNA (SQ) (ng) × 6.022×10^{23})/(Length of target genes (bp) × $660 \times 1 \times 10^{9}$) (Whelan et al. 2003), where SQ is the average of three technical replicates of the starting concentration (ng) value generated with software (CFX Maestro) and 6.022×10^{23} is Avogadro's constant. We also consider the conversion factor of 10^{9} and the average mass of 1 bp dsDNA, which is 660.

Sequence data was processed with software (Qiime2 version 2020.8) (Bolyen et al. 2019). Primers were removed using cutadapt (Martin 2011) before chimeric and low-quality regions were filtered out to produce Amplicon Sequence Variants (ASVs; DADA2 version 2020.8) (Bolyen et al. 2019). Taxonomy was assigned to each ASV using software (SILVA version 132) for bacteria (Yilmaz et al. 2014) and fungi (unite version 8.2) (Abarenkov et al. 2020). We excluded bacterial sequences assigned to mitochondria and chloroplasts, as well as fungal sequences that were not assigned to Kingdom Fungi. We assigned fungal ASVs to functional guilds using the FUNGuild database (Nguyen et al. 2016). Only ASVs with a "highly probable" confidence score are classified; all other ASVs are listed as "not classified."

2.7 | Statistical Analyses

We used linear mixed effect models (lme4 package in R; Bates et al. 2015) with ash depth as the predictor variable to test if soil burn severity affected initial soil POC and MAOC concentrations 17 days after burning. The models included MAOC or POC as dependent variables and plot and soil series as random effects to account for sampling design and potential differences between soil classifications. We plotted model residuals to ensure that they were normally distributed and ran simulation-based dispersion tests to assess if data were over-dispersed (Hartig and Lohse 2021); the linear models on untransformed variables passed both of these checks. We used the "anova" function to calculate F values, Satterthwaite's degrees of freedom, and statistical significance ($p < 0.05$; "lmerTest" package in R; Kuznetsova et al. 2017). A linear mixed-effect model was also used to assess if bulk density differed between burned and unburned plots 25 days after the fire. Plot and soil series were included as random effects.

We used a similar linear mixed effect modeling approach to assess how various dependent variables (POC, MAOC, PyOM-C, bacterial abundance, fungal abundance, bacterial richness, fungal richness, relative abundance of fungal guilds, extracellular enzyme activity, MAOC and POC $\delta^{13}C$ values, and leaf litter decomposition rates) differed between burned and unburned plots over time after the fire. Models included fire, time, and the interaction between fire and time as fixed predictor variables. Plot and soil series were included as random effects to account for the sampling design. We also included a unique identification for each subplot as a random effect to account for repeated measures. We plotted model residuals to ensure that they were normally distributed and ran simulation-based dispersion tests to assess if data were over-dispersed (Hartig and Lohse 2021); potential activity of BG, NAG, and phenol extracellular enzymes was log transformed to meet assumptions of normality. The "anova" function was used to assess which predictor variables were statistically significant, as described above (Kuznetsova et al. 2017).

The effects of fire and time on bacterial and fungal community composition were assessed using permutational analysis of variance (PERMANOVA) with the "adonis" function (vegan package in R; Oksanen et al. 2013). A blocking term was included using the "strata" argument to account for repeatedly measuring the same locations. The PERMANOVA was run on a dissimilarity matrix created using the "avgdist" function in R (Oksanen et al. 2013). The matrix used the Bray–Curtis dissimilarity index and reported median distances after 100 iterations. We also used this dissimilarity matrix to conduct principal coordinates analysis (PCoA; wcmdscale function; Oksanen et al. 2013). Scores from the first and second PCoA axes were plotted to visualize community composition, and scores from the first PCoA axis were included in models predicting POC and MAOC concentration (see below).

We used a model selection method to determine how microbial activity affected soil POC and MAOC in burned plots. Linear mixed-effect models contained potential activity of all eight extracellular enzymes as predictor variables and either POC or MAOC as response variables. We also ran separate models with fungal abundance, fungal richness, bacterial abundance, bacterial richness, fungal community composition (PCoA axis one), and bacterial community composition (PCoA axis one) as predictor variables. We did not run similar models including plant cover as predictor variables because we were unable to measure plant cover at the same time when soils were collected for analysis due to logistical constraints. All models included sampling plot, soil series, and sampling location as random effects to account for study design and repeated measures. To decide which predictor variables were significant, we compared all possible models after dropping each fixed term with a likelihood-ratio test (drop1 function in R) (R Core Team 2023; Tredennick et al. 2021).

3 | Results

3.1 | Soil C Pools: POC, MAOC, C:N, PyOM-C, and $\delta^{13}C$

On average, fire decreased POC by ~3 times in burned (17.7 ± 1.78 g C kg^{-1} soil; mean ± standard error) compared to unburned plots (46.5 ± 8.36 g C kg^{-1} soil). POC continued to decrease from 25.5 ± 5.67 g C kg^{-1} soil 17 days to 15.0 ± 2.02 g C kg^{-1} soil 4 years after the fire in burned plots (fire by time interaction $F_{1,60} = 59.8$, $p = 0.03$; Figure 1A). Fire also decreased MAOC, but only by ~0.3 times in burned (6.23 ± 0.44 g C kg^{-1} soil) compared to unburned plots (9.26 ± 0.87 g C kg^{-1} soil; time by fire interaction $F_{1,49} = 7.52$, $p = 0.008$). In contrast, MAOC did not change over time in the burned plots (6.31 ± 0.92 g C kg^{-1} soil 17 days versus 6.32 ± 0.87 g C kg^{-1} soil 4 years after the fire), and the significant time by fire interaction was likely driven by variation in the unburned plots (Figure 1B). Neither MAOC ($p = 0.13$) nor POC ($p = 0.64$) was explained by ash depth—used as an index of fine-scale soil burn severity—in burned plots (Figure S2). Ash depth ranged from 0.5 to 8.25 cm and averaged 4.70 ± 2.56 cm standard deviation in the burned plots 17 days after the fire, reaching the > 3 cm threshold that qualifies as high burn severity in 8 out of 12 subplots (Parsons et al. 2010).

When bulk density was used to estimate soil C stocks, POC followed similar trends but was only 1.6 times lower in burned plots (14.3 ± 10.7 Mg-C ha^{-1}) than in unburned plots (23.5 ± 19.9 Mg-C ha^{-1}). However, fire did not consistently deplete MAOC stocks calculated with bulk density (Figure S3). We note that fire increased bulk density to 0.82 ± 0.16 g soil cm^{-3} in burned plots compared to 0.56 ± 0.17 g soil cm^{-3} in control plots ($p = 0.001$), and soil compaction may explain why POC and MAOC stocks did not respond as strongly to fire as C did on a per mass basis.

Fire increased POC $\delta^{13}C$ values in burned plots (−27.5‰ ± 0.15‰) compared to unburned plots (−28.2‰ ± 0.17‰; fire effect $F_{1,16} = 5.78$, $p = 0.028$; Figure 2A). Like POC, $\delta^{13}C$ in MAOC slightly increased between 17 days (−26.4‰ ± 0.56‰) and 4 years (−26.2‰ ± 0.44‰) after the fire in the burned plots and

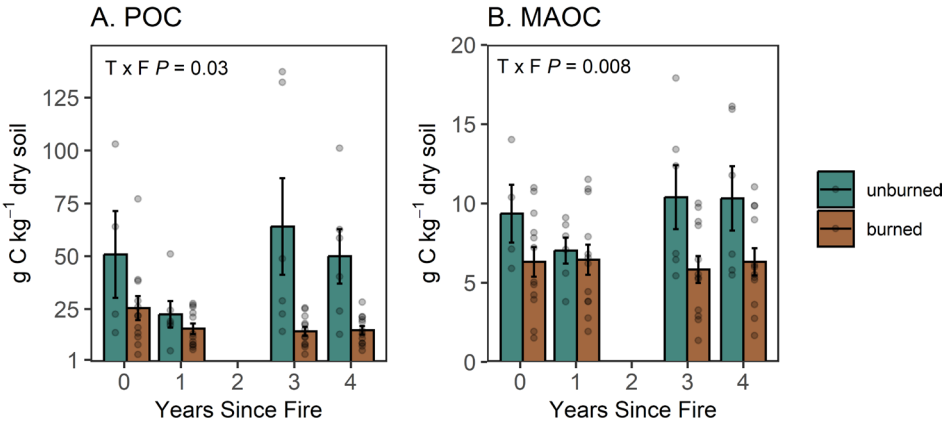

FIGURE 1 | Soil C concentrations in (A) particulate organic carbon (POC) and (B) mineral-associated organic carbon (MAOC) measured in surface soils (0–10 cm). Colors represent whether soils were collected from burned (brown) or unburned (green) plots. Bars correspond to mean carbon concentrations ($N = 6$ for unburned and 12 for burned), error bars represent one standard error of the mean, and dots represent individual measurements. *p* values show results from linear mixed effects models; T = effect of time, F = effect of fire, and T × F = interaction effect of time and fire.

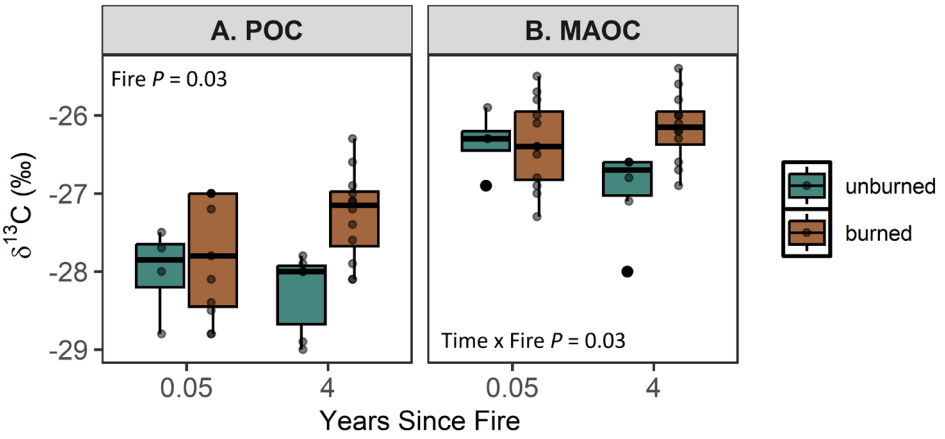

FIGURE 2 | Isotopic composition ($\delta^{13}C$) of C in (A) particulate organic matter (POC) and (B) mineral-associated organic matter (MAOC), collected either 17 days (0.05 years) and 1460 days (4 years) post-fire. Colors represent whether soils were collected from burned (brown) or unburned (green) plots. Horizontal lines within each box represent the median ($N = 6$ for unburned and 12 for burned), the upper and lower bounds of the box represent the interquartile range, vertical lines represent the largest and smallest values within 1.5 times of the interquartile range, shaded black dots represent individual measurements, and solid black dots represent outliers. *p* values show results from linear mixed effects models.

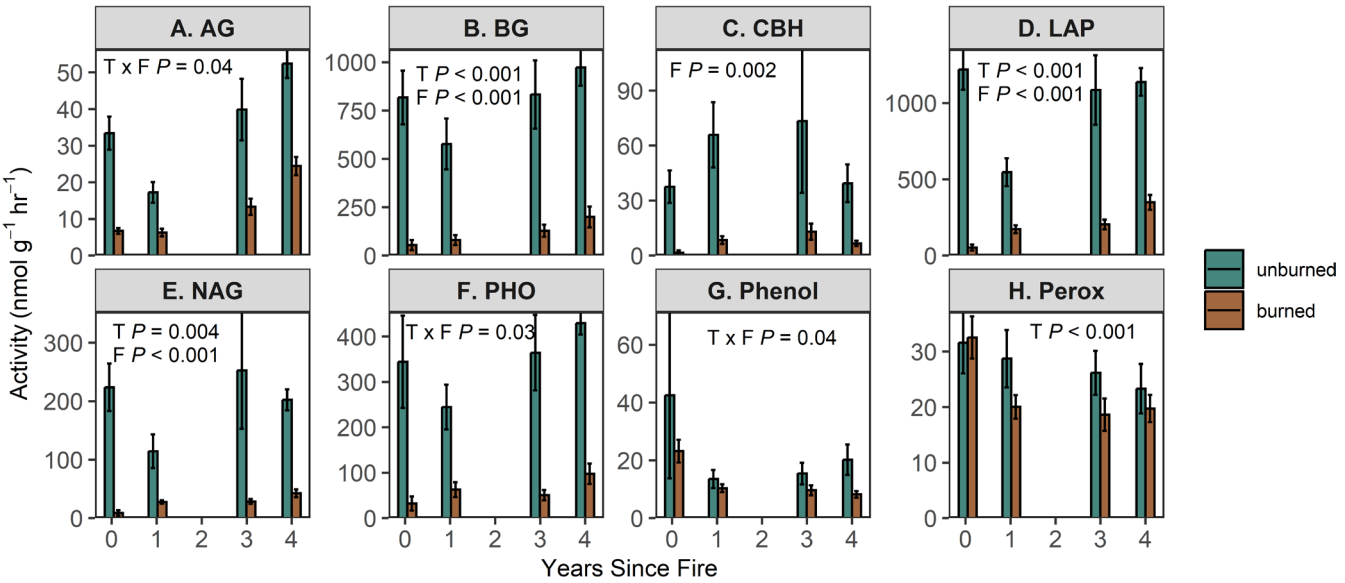

FIGURE 3 | Soil potential extracellular enzyme activity of (A—D) hydrolytic enzymes involved in C degradation (AG, BG, CBH, LAP), (E) a hydrolytic enzyme involved in N acquisition (NAG), (F) a hydrolytic enzyme involved in P acquisition (PHO), and (G, H) oxidative enzymes involved in C degradation (Phenol and Perox). Enzyme activity was measured in surface soils (0–10 cm) from burned (brown) and unburned (green) plots. Bars correspond to mean activity ($N = 6$ for unburned and 12 for burned), error bars represent one standard error of the mean, and dots represent individual measurements. p values show results from linear mixed effects models; T = effect of time, F = effect of fire, and T × F = interaction effect of time and fire.

decreased by 0.6‰ during this same time in unburned plots (fire by time interaction $F_{1,13} = 12.6$, $p = 0.031$; Figure 2B).

Fire decreased the C:N ratio of MAOC in burned plots, whereas in unburned plots, the C:N ratio of MAOC increased over time (fire by time interaction $F_{1,5} = 4.78$, $p = 0.034$; Figure S4). The difference between the C:N ratio in burned versus unburned plots increased from 17 days after burning (when C:N was 1.3 times greater in unburned plots compared to burned plots) to 3 years after burning (when C:N was 1.5 times greater in unburned plots compared to burned plots). While the C:N ratio of POC did not differ between burned and unburned soils ($p = 0.79$), it did change over time ($F_{1,52} = 16.2$, $p < 0.001$), decreasing from an average of 30.3 ± 3.1 17 days after the fire to 20.4 ± 0.5 4 years.

PyOM-C was consistently lower in burned than in unburned plots 17 days, 2 years, and 4 years after burning (fire main effect $F_{1,6} = 20$, $p = 0.004$). Including all time points, PyOM averaged 3.09 ± 0.29 g C kg^{-1} dry soil in burned plots compared to 7.01 ± 0.44 g C kg^{-1} dry soil in unburned plots (Figure S5).

3.2 | Potential Extracellular Enzyme Activity and Field Litter Decomposition Rates

Fire reduced the potential activity of all hydrolytic extracellular enzymes relative to unburned plots (fire main effect $p < 0.01$; Figure 3A–F). Potential activity of the C-acquiring enzyme AG increased over time in burned plots compared to unburned plots (fire by time interaction $F_{1,44} = 4.38$, $p = 0.042$; Figure 3A), as did the activity of the P-acquiring enzyme PHO (fire by time interaction $F_{1,43} = 4.95$, $p = 0.031$; Figure 3F). Potential activity of the C-acquiring enzyme β-glucosidase ($F_{1,42} = 15.3$, $p < 0.001$; Figure 3B), the N-acquiring enzyme LAP ($F_{1,42} = 12.8$, $p < 0.001$; Figure 3D), and the N-acquiring enzyme NAG ($F_{1,51} = 9.04$, $p = 0.004$; Figure 3E) increased over time in burned plots.

Phenol oxidase activity was lower in burned than in unburned plots and decreased over time in burned plots (fire by time interaction $F_{1,49} = 4.59$, $p = 0.037$; Figure 3G). While fire did not affect the activity of peroxidase ($p = 0.61$), peroxidase activity decreased over time in both burned and unburned plots (time main effect $F_{1,35} = 14.4$, $p < 0.001$; Figure 3H).

Using model selection, we found that POC concentrations in burned plots were negatively associated with the potential activity of AG ($p = 0.01$), CBH ($p = 0.04$), and PHO ($p = 0.01$), and positively associated with BG ($p = 0.01$). MAOC concentrations were negatively associated with AG activity ($p = 0.001$) and positively associated with LAP activity ($p = 0.012$; Table 1).

Mass loss of ground *A. glandulosa* litter did not differ between burned and unburned plots ($F_{1,7} = 6.89$, $p = 0.14$; Figure S6). In general, litter mass loss increased with incubation time ($F_{2,60} = 13.6$, $p < 0.001$).

3.3 | Recovery of Plant Communities

Fire decreased the cover of shrubs (fire by time interaction $F_{1,174} = 4.07$, $p = 0.045$), the dominant shrub *A. glandulosa* (fire effect $F_{1,8} = 22.9$, $p = 0.001$), as well as plant litter (fire by time interaction $F_{3,102} = 12.4$, $p < 0.001$; Figure 4). In burned plots, percent cover of all shrubs increased from 6.83% ± 1.91% at 286 days to 47.4% ± 9.57% at 1314 days (3.6 years) after the fire (Figure 4A). Percent cover of *A. glandulosa* increased from 3.85% ± 1.60% at 286 to 16.0% ± 5.39% at 1314 days (3.6 years) after the fire in burned plots, and from 49.0% ± 10.3% to 66.7% ± 12.8% in unburned plots

TABLE 1 | Results from linear mixed-effect models predicting POC and MAOC concentrations based on extracellular enzyme activity.

Dependent variable	Fixed variables	Estimate	SE	*t*	Drop1 *p* value
POC	AG	−0.30	0.11	−2.70	**0.01**
	BG	0.03	0.01	2.71	**0.01**
	CBH	−0.26	0.12	−2.15	**0.04**
	NAG	0.04	0.09	0.46	0.65
	LAP	0.02	0.01	1.25	0.23
	PHO	−0.09	0.03	−2.59	**0.01**
	Phenol	0.09	0.13	0.70	0.49
	Peroxidase	0.11	0.14	0.77	0.45
MAOC	AG	−0.10	0.024	−4.10	**0.001**
	BG	0.00	0.003	0.77	0.45
	CBH	−0.05	0.025	−1.89	0.08
	NAG	0.02	0.020	0.96	0.35
	LAP	0.01	0.003	2.81	**0.01**
	PHO	−0.00	0.006	−0.04	0.56
	Phenol	0.05	0.029	1.56	0.14
	Peroxidase	−0.01	0.031	−0.35	0.56

Note: All soil potential extracellular enzyme activities were initially included as fixed effects. Values represent model coefficients, standard error (SE), and *t* values assessed using the "Anova" function in R. The *p* values indicate if each fixed variable is statistically significant compared to a series of models run without that variable, as assessed using the drop1 function in R; bold values are statistically significant ($p < 0.05$).
Abbreviations: AG = α-glucosidase, BG = β-glucosidase, CBH = 1,4-β-cellobiohydrolase, LAP = l-leucine aminopeptidase, NAG = *N*-acetyl-β-D-glucosaminidase, peroxidase = peroxidase, phenol = phenol oxidase, PHO = phosphomonoesterase.

(time main effect $F_{1,4} = 47.5$, $p = 0.001$; Figure 4B). Plant litter cover increased from 3.96% ± 0.55% at 286 days to 18.2% ± 3.03% at 1314 days (3.6 years) after the fire in burned plots (Figure 4D).

In contrast to shrubs and plant litter, fire increased the percent cover of subshrubs (fire by time interaction $F_{1,174} = 8.96$, $p = 0.003$; Figure 4C) and herbs (fire effect $F_{1,18} = 5.05$, $p = 0.037$; Figure 4E). Subshrub cover in burned plots increased from 1.58% ± 0.14% at 286 days after the fire to 16.3% ± 4.49% at 1314 days (3.6 years); subshrub cover was always below 1% in unburned plots (Figure 4C). Herb cover averaged 4.69% ± 0.78% in burned compared to 0.61% ± 0.35% in unburned plots. The only grass we identified was *Bromus madretensis rubens*, which averaged below 1% cover regardless of fire (Figure 5F).

Shrub leaf $\delta^{13}C$ values did not differ between the two dominant shrubs, but did differ based on regeneration stage ($F_{2,24} = 18.9$, $p < 0.001$; Figure S7). Adult leaves were most enriched in $\delta^{13}C$ (−27.6‰ ± 0.23‰) compared to resprouter (−29.0‰ ± 0.20‰) or seedling (−30.1‰ ± 0.4‰) leaves.

3.4 | Fungal and Bacterial Abundance, Species Richness, and Community Composition

Fire significantly reduced both bacterial and fungal abundance, and neither recovered to unburned levels by 4 years post-fire. Fire initially reduced bacterial abundance, but bacterial abundance increased over time in burned plots (fire by time interaction $F_{1,52} = 10.1$, $p = 0.003$; Figure 5A). Seventeen days after the fire, bacterial abundance was 16 times higher in unburned ($1.5 \times 10^{10} \pm 4.46 \times 10^{9}$ copy numbers g^{-1} soil) than burned plots ($9.32 \times 10^{8} \pm 4.33 \times 10^{8}$ copy numbers g^{-1}; Figure 5A). Four years after the fire, bacterial abundance was only ~3.5 times higher in unburned ($2.65 \times 10^{10} \pm 5.22 \times 10^{9}$ copy numbers g^{-1} soil) than burned plots ($7.40 \times 10^{9} \pm 1.41 \times 10^{9}$ copy numbers g^{-1}). Like bacteria, fire also decreased fungal abundance, which increased over time in burned plots (fire by time interaction $F_{1,57} = 12.9$, $p < 0.001$; Figure 5B). Seventeen days after the fire, fungal abundance was over 48 times higher in unburned ($1.55 \times 10^{9} \pm 3.88 \times 10^{8}$ copy numbers g^{-1} soil) than in burned plots ($3.21 \times 10^{7} \pm 1.65 \times 10^{7}$ copy numbers g^{-1}). Four years after the fire, fungal abundance was over five times higher in unburned ($1.07 \times 10^{9} \pm 2.61 \times 10^{8}$ copy numbers g^{-1} soil) than burned plots ($2.04 \times 10^{8} \pm 4.26 \times 10^{7}$ copy numbers g^{-1}).

Bacterial species richness changed over time ($F_{1,55} = 4.86$, $p = 0.03$), but did not differ between burned and unburned plots ($F_{1,36} = 0.80$, $p = 0.38$; Figure 5C). Regardless of fire, bacterial species richness was highest 3 years after the fire (818 ± 90.4 ASVs) and lowest 1 year after the fire (427 ± 36.7 ASVs). Unlike bacteria, the fungal species richness was consistently lower in the burned plots ($F_{1,19} = 10.2$, $p = 0.005$) and did not change over time ($F_{1,43} = 0.27$, $p = 0.61$), averaging 283 ± 18.6 ASVs in unburned plots compared to 122 ± 9.73 ASVs in burned plots (Figure 5D).

Bacterial and fungal community composition was distinct between burned and unburned plots and changed over time

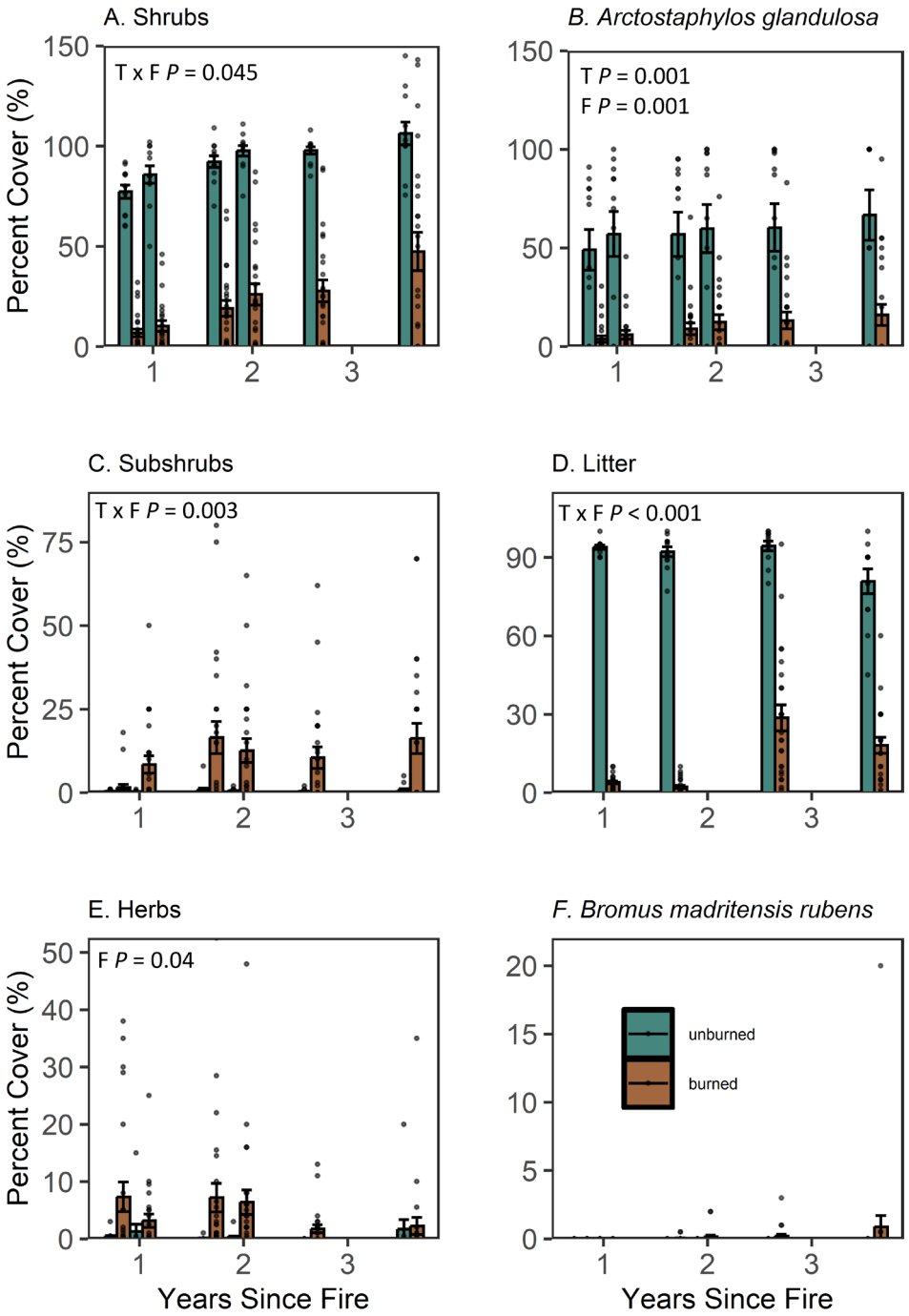

FIGURE 4 | Percent plant cover of (A) all shrubs, (B) Manzanita (*Arctostaphylos glandulosa*), (C) all subshrubs, (D) leaf litter, (E) all herbs, and (F) Red brome (*Bromus madreitensis rubens*) measured in burned (brown) and unburned (green) plots during the first 5 years post-fire. Bars correspond to mean percent cover, error bars represent one standard error of the mean, and dots represent individual measurements. *p* values show results from linear mixed effects models; T = effect of time, F = effect of fire, and T × F = interaction effect of time and fire.

in the burned plots (bacteria: adonis2 time by fire interaction $F_{3,57} = 1.46$, $p = 0.01$; fungi: time by fire interaction $F_{3,55} = 1.55$, $p = 0.01$; Figure S8). Fire significantly decreased the abundance of taxa classified as ectomycorrhizal fungi (EMF; based on highly probable FUNGuild classifications; $F_{1,26} = 25.3$, $p < 0.001$) from 48% in control plots to 15% in burned plots (Figure S9).

Both bacterial and fungal community composition (assessed using PCoA axis scores) was associated with POC in burned soils (Table 2); this was not the case for fungal or bacterial abundance or species richness. No microbial indices were associated with MOAC in burned soils (Table 2).

4 | Discussion

We monitored soil POC, MAOC, PyOM-C, microbial activity, microbial community composition, and plant cover, starting 17 days after a 94-km^2 wildfire burned a southern California

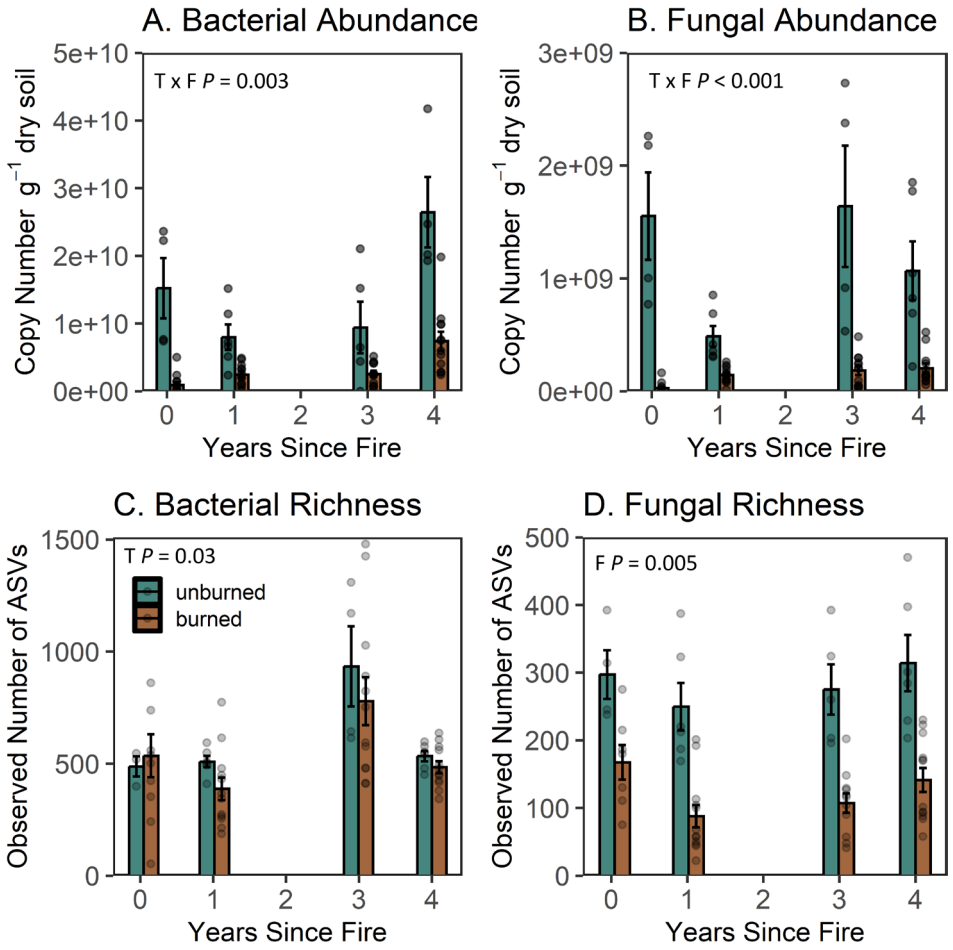

FIGURE 5 | Abundance of (A) soil bacteria and (B) soil fungi based on quantitative polymerase chain reaction (qPCR) copy number as well as species richness of (C) bacteria and (D) fungi based on observed amplicon sequence variants (ASVs). Microbial communities were measured in surface soils (0–10 cm) from burned (brown) and unburned (green) plots. Bars represent the mean ($N = 6$ for unburned and 12 for burned), error bars represent one standard error of the mean, and dots represent individual measurements. *p* values show results from linear mixed effects models; T = effect of time, F = effect of fire, and T × F = interaction effect of time and fire.

shrubland, to understand controls over soil C loss and accumulation in burned ecosystems. We found that fire immediately decreased POC by 50% and MAOC by 33%, supporting the hypothesis that MAOC is more resistant to volatilization than POC (H1). However, neither POC nor MAOC decreased as a function of ash depth, contrary to our hypothesis that higher soil burn severity would volatilize more soil C (H2). In the post-fire environment, POC continued to decrease for 1 year by another 38%, coinciding with the recovery of microbial abundance and extracellular enzyme activity, supporting the hypothesis that microbial decomposition would initially outpace plant C inputs to the soil and, thus, lower POC (H3). However, after this initial decrease in POC, both POC and MAOC pools remained relatively unchanged between 1 and 4 years post fire, suggesting that microbial respiration and plant C inputs were in equilibrium. Altogether, our observations suggest that wildfires can lower chaparral soil C pools, not only because wildfires directly combusted about half of the POC and one third of the MAOC at our site, but also because it may take more than 4 years for plant C inputs to outpace C losses via microbial respiration.

4.1 | How Do Minerals and Soil Burn Severity Affect Initial Soil C Loss After Wildfire?

Severe wildfires may burn hot enough to combust C in mineral surface soils, helping to explain why POC, MAOC, and PyOM-C all decreased just 17 days after the fire. While it is possible both microbial respiration and erosion may have contributed to this initial C loss we attribute to combustion (Berhe and Kleber 2013; Berhe et al. 2018), their contributions would have been small as fire decreased the abundance of both bacteria and fungi by 95% (Figure 4) and it still had not rained at our site to favor erosion. Of the C that remained in soils, mineral associations likely offered protection against combustion (fire decreased MAOC by only 33% whereas it decreased POC by 50%), even in these sandy, relatively MAOC-poor soils, consistent with lab observations that MAOC is more resistant to combustion than POC (Merino et al. 2021; Wang et al. 2023). The fire also combusted 50% of PyOM-C, a surprising finding given that PyOM originates from burning. It has been suggested that wildfires may burn hot enough to volatilize PyOM-C formed from prior fires (DeLuca et al. 2020; Hatten

TABLE 2 | Results from linear mixed-effect models predicting POC and MAOC concentrations in burned soils based on microbial community composition.

Dependent variable	Fixed variables	Estimate	SE	*t*	Drop1 *p* value
POC	Bacteria copy number	2.10	2.68	0.78	0.44
	Fungal copy number	−1.03	2.44	−0.42	0.68
	Bacteria richness	0.58	1.97	0.29	0.77
	Fungi richness	3.34	3.20	1.05	0.30
	Bacteria PCoA axis 1	10.8	4.82	6.40	**0.032**
	Fungi PCoA axis 1	−11.6	4.17	−2.24	**0.009**
MAOC	Bacteria copy number	0.32	0.37	0.88	0.39
	Fungal copy number	0.53	0.34	1.56	0.12
	Bacteria richness	−0.067	0.45	−0.24	0.81
	Fungi richness	−0.33	0.28	−0.74	0.47
	Bacteria PCoA axis 1	0.18	0.69	0.26	0.80
	Fungi PCoA axis 1	−0.58	0.59	−0.91	0.33

Note: Bacterial and fungal richness, abundance, and community composition (PCoA axis one score) were initially included as fixed effects. Values represent model coefficients, standard error (SE), and *t* values assessed using the Anova function in R. The *p* values indicate if each fixed variable is statistically significant compared to a series of models run without that variable, as assessed using the drop1 function in R; bold values are statistically significant ($p < 0.05$).

et al. 2008), but other methods, such as nuclear magnetic resonance may be necessary to best identify PyOM that is resistant to burning (Chatterjee et al. 2012). Together, these C losses measured 17 days after the fire appeared consistent with our hypothesis that more severe burning would deplete more soil C. However, when we used ash depth to estimate the impacts of fine-scale soil burn severity on soil C stocks, neither POC, MAOC, nor PyOM-C were associated with ash depth ranging from low (< 1 cm) to high (> 3 cm) severity, contradicting our hypothesis. It is possible the fire may have burned severely enough to volatilize C regardless of fine-scale burn severity. Regardless, our results show that shrubland fires can volatilize much surface mineral C, a C loss pathway that has primarily been documented in mesic systems with organic-rich soils (Pellegrini et al. 2023; Walker et al. 2019; Wardle et al. 2003). Furthermore, POC and PyOM-C were both more sensitive to burning than MAOC, suggesting that MAOC may be the most persistent form of C in this Mediterranean shrubland.

4.2 | How Does the Recovery of Plants and Microorganisms Affect Soil C Pools After Wildfire?

During the first few months after the wildfire was extinguished, the recovery of microbial C respiration, without a concomitant increase in photosynthetic C inputs, may have been a key mechanism lowering POC. In addition to respiration, erosion of surface soil could also have exposed deeper soils that were depleted in C, contributing to the loss of POC we measured in the first year post fire (Abney et al. 2017; Berhe et al. 2018). While our study was not designed to quantify erosion, depositional areas at a mixed conifer site in the Sierra Nevada, CA, USA, gained ~4 mg g^{-1} POC one year post fire (Abney et al. 2017), suggesting erosion could have contributed to the 11 mg g^{-1} POC loss we measured. However, the 38% decrease in POC between 17 days and one year post fire corresponded to an increase in bacterial and fungal abundance at our site, suggesting that microbial respiration also lowered POC (Figure 5). These recovering microbial communities produced extracellular enzymes targeting C degradation (AG and CBH), generating an inverse relationship with POC in burned soils. This net loss of POC suggests that microbial C respiration was not balanced by photosynthetic C inputs, despite the initial recovery of shrubs between 17 days and one year after fire and the higher abundance of herbs and subshrubs in burned than in unburned plots. It is possible that vegetation recovery relied more on "auto-succession," where the pre-fire shrubs resprout and gradually establish dominance (Hanes 1971), which is a longer process than the relatively rapid growth of early colonizing and fire-resistant microorganisms (Pulido-Chavez et al. 2022; Whitman et al. 2019) that can drive decomposition in burned soils (Pellegrini, Caprio, et al. 2021; Q. Wang et al. 2012). Indeed, fungal and bacterial community composition not only began to recover relatively quickly, but they (PCoA axis 1) were associated with soil POC (Table 2), suggesting that fast-growing and fire-resistant fungi and bacteria decomposed POC during the first year following the fire, contributing to C losses that outpaced photosynthetic C inputs.

One to four years after the fire was extinguished, shrub and leaf litter cover increased, but these new plant C inputs must still not have been enough to exceed microbial C demand or losses to erosion, as soil C pools did not increase. This dominance of microbial decomposition over plant C inputs is consistent with the observed enrichment in soil $\delta^{13}C$ values, as plant-derived C with lighter $\delta^{13}C$ values likely made up a smaller portion of total C compared to the more $\delta^{13}C$-heavy microbial-derived C, enriching soils with ^{13}C in burned plots where plant C inputs could not outpace microbial decomposition. While the higher

soil $\delta^{13}C$ we measured after the fire could have been caused by a shift from C3 to C4 plants as grasses invade burned landscapes (Pellegrini et al. 2023), we saw no evidence for this at our site (Figure 4), suggesting that the shift in soil $\delta^{13}C$ was due to fewer plant-derived C inputs. Furthermore, microbial contributions to bulk soil $\delta^{13}C$ values are consistent with the similar decomposition rates of *A. glandulosa* leaf litter measured in burned and unburned plots (Figure S6), suggesting microbial activity remained high despite substantial changes in their community composition. Low inputs of plant organic matter can also limit soil N availability, encouraging microbes to find other sources of N, like MAOM (Daly et al. 2021; Jilling et al. 2018). MAOM may have been a substantial source of N in our burned soils, where heating decreased its C:N ratio, likely through the Maillard reaction pathway (the formation of N-rich molecules from the heating of polysaccharides and proteins; Bahureksa et al. 2022; VanderRoest et al. 2024; Figure S4). Consistent with this understanding, LAP activity—an enzyme produced to acquire N—was positively associated with MAOC in burned plots, suggesting that microbes may have produced more enzymes to access mineral-bound N in burned soils. Taken together, our results support the conclusion that while plant growth began to recover within 1–4 years after the fire, plant organic matter inputs did not meet microbial C and nutritional demands, slowing the recovery of soil C pools.

Plant growth and associated photosynthetic C inputs to the soil must outpace microbial C demands before soil C pools can recover from wildfire-induced losses. At our site, plant C inputs to the soil were likely limited in burned plots where the cover of *A. glandulosa* remained ~3 times lower than in unburned plots 4 years after the fire. While shrubs could increase belowground C allocation without increases in their aboveground cover, the enrichment of soil $\delta^{13}C$ we measured suggests that plant C inputs declined in burned soils; new plant C inputs would be expected to lower $\delta^{13}C$ soil values. Soil C may remain depleted if future fire return intervals—which are historically 30–90 years in California chaparral (USDA, Forest Service, Missoula Fire Sciences Laboratory 2018)—become shorter than the 10–30 years it may take for shrubs to fully recover and increase soil C inputs (O'Leary 1984; Vogl and Schorr 1972). In addition to directly limiting belowground C inputs, slowed plant recovery may adversely affect ectomycorrhizal fungi (ECM), which are major components of SOM (Högberg et al. 2020; Schweigert et al. 2015). We found that fungal abundance and richness remained depleted in burned soils even after 4 years (Figure 5), partially reflecting limited recovery of the ECM that can be associated with *A. glandulosa* (Figure S9; Allen et al. 1999; Plamboeck et al. 2007). While an increased abundance of saprotrophic fungi that decompose plant litter or PyOM could also help build soil C pools (Floudas et al. 2012; Huang et al. 2022; Riley et al. 2014), similar decomposition rates of *A. glandulosa* litter between burned and unburned plots suggest the fire did not hinder decomposer activity. Despite the partial recovery of plant cover and ECM abundance in burned plots between 1- and 4-years post-fire, soil C pools did not increase, suggesting that plant and fungal C inputs must continue to recover before they outpace losses from microbial respiration.

5 | Conclusion

We tracked the trajectory of soil C pools, litter decomposition, and microbial and plant communities over 4 years to understand the fate of soil C following a chaparral wildfire. We found that fire can deplete roughly half of the surface soil C pools, largely due to the susceptibility of POC to combustion. While microbial decomposition further depleted soil POC during the first year following the fire, POC and MAOC did not change between 1 and 4 years after the fire, suggesting that C losses controlled by microbes were in equilibrium with plant C inputs to the soil. Our results suggest that supporting the recovery of dominant shrubs and their associated mycorrhizal fungi may help promote belowground C inputs in our chaparral ecosystem. Otherwise, plant C inputs to the soil may be outpaced by C losses from combustion and decomposition as climate change increases wildfire frequency and severity, increasing the turnover of soil C.

Author Contributions

Alexander H. Krichels: conceptualization, data curation, formal analysis, investigation, methodology, project administration, supervision, validation, visualization, writing – original draft, writing – review and editing. **Elizah Z. Stephens:** data curation, investigation, methodology, visualization, writing – review and editing. **Chloe Reid:** data curation, investigation, methodology, project administration, writing – review and editing. **M. Fabiola Pulido Barriga:** conceptualization, data curation, investigation, methodology, visualization, writing – review and editing. **Maria E. Ordoñez:** data curation, methodology, writing – review and editing. **Jennie R. McLaren:** methodology, validation, writing – review and editing. **Meg Kargul:** investigation, data curation, methodology, writing – review and editing. **Loralee Larios:** investigation, data curation, methodology, project administration, resources, supervision, validation, writing – review and editing. **Sydney I. Glassman:** conceptualization, funding acquisition, investigation, methodology, project administration, resources, supervision, writing – review and editing. **Peter M. Homyak:** conceptualization, funding acquisition, investigation, methodology, project administration, resources, supervision, writing – review and editing.

Acknowledgments

We thank Darrel Vance, Emily Fudge, Jeffrey Heys, Lauren Quon, Jacob Rodriguez, and Victoria Stempniewicz from the Cleveland National Forest and the Trabuco Ranger District for their guidance and help with permitting and site selection. We also thank Aral C. Greene, Ariana Firebaugh Ornelas, Johann Püspök, Judy A. Chung, James Randolph, Dylan Enright, Taylor Naquin, Clarissa S. Rodriguez, Sameer S. Saroa, Stuart Schwab, Noah Teller, and Stephanie Tyler for their help with field and lab work. This work was funded by the United States Department of Agriculture (USDA; NIFA Award #2022-67014-36675) and Department of Energy (DOE; DE-SC0023127) grants to Sydney I. Glassman and Peter M. Homyak, the United States National Science Foundation grant to Peter M. Homyak (DEB 1916622), and supported in part by the USDA Forest Service Rocky Mountain Research Station. The findings and conclusions in this publication are those of the authors and should not be construed to represent any official USDA or U.S. Government determination or policy.

Conflicts of Interest

The authors declare no conflicts of interest.

Data Availability Statement

The data that support the findings of this study are openly available in Dryad at https://doi.org/10.5061/dryad.tx95x6b76. Raw sequence reads are available under BioProject accession number PRJNA761539 at https://www.ncbi.nlm.nih.gov/sra/PRJNA761539.

References

Abarenkov, K., A. Zirk, T. Piirmann, et al. 2020. "UNITE QIIME Release for Fungi 2." https://doi.org/10.15156/BIO/786387.

Abatzoglou, J. T., A. P. Williams, and R. Barbero. 2019. "Global Emergence of Anthropogenic Climate Change in Fire Weather Indices." *Geophysical Research Letters* 46, no. 1: 326–336. https://doi.org/10.1029/2018GL080959.

Abney, R. B., J. Sanderman, D. Johnson, M. L. Fogel, and A. A. Berhe. 2017. "Post-Wildfire Erosion in Mountainous Terrain Leads to Rapid and Major Redistribution of Soil Organic Carbon." *Frontiers in Earth Science* 5: 99. https://doi.org/10.3389/feart.2017.00099.

Allen, M. F., L. M. Egerton-Warburton, E. B. Allen, and O. Kårén. 1999. "Mycorrhizae in *Adenostoma fasciculatum* Hook. & Arn.: A Combination of Unusual Ecto- and Endo-Forms." *Mycorrhiza* 8, no. 4: 225–228. https://doi.org/10.1007/s005720050238.

Ansley, R. J., T. W. Boutton, and J. O. Skjemstad. 2006. "Soil Organic Carbon and Black Carbon Storage and Dynamics Under Different Fire Regimes in Temperate Mixed-Grass Savanna." *Global Biogeochemical Cycles* 20, no. 3: GB3006. https://doi.org/10.1029/2005gb002670.

Bahram, M., U. Kõljalg, P.-E. Courty, et al. 2013. "The Distance Decay of Similarity in Communities of Ectomycorrhizal Fungi in Different Ecosystems and Scales." *Journal of Ecology* 101, no. 5: 1335–1344. https://doi.org/10.1111/1365-2745.12120.

Bahureksa, W., R. B. Young, A. M. McKenna, et al. 2022. "Nitrogen Enrichment During Soil Organic Matter Burning and Molecular Evidence of Maillard Reactions." *Environmental Science & Technology* 56, no. 7: 4597–4609. https://doi.org/10.1021/acs.est.1c06745.

Bates, D., M. Mächler, B. Bolker, and S. Walker. 2015. "Fitting Linear Mixed-Effects Models Using lme4." *Journal of Statistical Software* 67: 1–48. https://doi.org/10.18637/jss.v067.i01.

Berhe, A. A., R. T. Barnes, J. Six, and E. Marin-Spiotta. 2018. "Role of Soil Erosion in Biogeochemical Cycling of Essential Elements: Carbon, Nitrogen, and Phosphorus." *Annual Review of Earth and Planetary Sciences* 46: 521–548.

Berhe, A. A., and M. Kleber. 2013. "Erosion, Deposition, and the Persistence of Soil Organic Matter: Mechanistic Considerations and Problems With Terminology: Som Stabilization in Eroding Landscapes." *Earth Surface Processes and Landforms* 38, no. 8: 908–912. https://doi.org/10.1002/esp.3408.

Bolyen, E., J. R. Rideout, M. R. Dillon, et al. 2019. "Reproducible, Interactive, Scalable and Extensible Microbiome Data Science Using QIIME 2." *Nature Biotechnology* 37, no. 8: 852–857. https://doi.org/10.1038/s41587-019-0209-9.

Camenzind, T., K. Mason-Jones, I. Mansour, M. C. Rillig, and J. Lehmann. 2023. "Formation of Necromass-Derived Soil Organic Carbon Determined by Microbial Death Pathways." *Nature Geoscience* 16: 115–122. https://doi.org/10.1038/s41561-022-01100-3.

Caporaso, J. G., C. L. Lauber, W. A. Walters, et al. 2011. "Global Patterns of 16S rRNA Diversity at a Depth of Millions of Sequences Per Sample." *Proceedings of the National Academy of Sciences of the United States of America* 108, no. Suppl 1: 4516–4522. https://doi.org/10.1073/pnas.1000080107.

Certini, G. 2005. "Effects of Fire on Properties of Forest Soils: A Review." *Oecologia* 143, no. 1: 1–10. https://doi.org/10.1007/s00442-004-1788-.

Chatterjee, S., F. Santos, S. Abiven, B. Itin, R. E. Stark, and J. A. Bird. 2012. "Elucidating the Chemical Structure of Pyrogenic Organic Matter by Combining Magnetic Resonance, Mid-Infrared Spectroscopy and Mass Spectrometry." *Organic Geochemistry* 51: 35–44. https://doi.org/10.1016/j.orggeochem.2012.07.006.

Cotrufo, M. F., M. G. Ranalli, M. L. Haddix, J. Six, and E. Lugato. 2019. "Soil Carbon Storage Informed by Particulate and Mineral-Associated Organic Matter." *Nature Geoscience* 12, no. 12: 989–994. https://doi.org/10.1038/s41561-019-0484-6.

Daly, A. B., A. Jilling, T. M. Bowles, et al. 2021. "A Holistic Framework Integrating Plant-Microbe-Mineral Regulation of Soil Bioavailable Nitrogen." *Biogeochemistry* 9: 211–229. https://doi.org/10.1007/s10533-021-00793-9.

DeBano, L. F. 2000. "The Role of Fire and Soil Heating on Water Repellency in Wildland Environments: A Review." *Journal of Hydrology* 231: 195–206. https://doi.org/10.1016/S0022-1694(00)00194-3.

DeLuca, T. H., M. J. Gundale, R. J. Brimmer, and S. Gao. 2020. "Pyrogenic Carbon Generation From Fire and Forest Restoration Treatments." *Frontiers in Forests and Global Change* 3: 24. https://doi.org/10.3389/ffgc.2020.00024.

Dooley, S. R., and K. K. Treseder. 2012. "The Effect of Fire on Microbial Biomass: A Meta-Analysis of Field Studies." *Biogeochemistry* 109, no. 1: 49–61. https://doi.org/10.1007/s10533-011-9633-8.

Dove, N. C., and S. C. Hart. 2017. "Fire Reduces Fungal Species Richness and In Situ Mycorrhizal Colonization: A Meta-Analysis." *Fire Ecology* 13, no. 2: 37–65. https://doi.org/10.4996/fireecology.130237746.

Ehleringer, J. R., N. Buchmann, and L. B. Flanagan. 2000. "Carbon Isotope Ratios in Belowground Carbon Cycle Processes." *Ecological Applications* 10, no. 2: 412–422. https://doi.org/10.1890/1051-0761(2000)010[0412:CIRIBC]2.0.CO;2.

Ekblad, A., H. Wallander, D. L. Godbold, et al. 2013. "The Production and Turnover of Extramatrical Mycelium of Ectomycorrhizal Fungi in Forest Soils: Role in Carbon Cycling." *Plant and Soil* 366, no. 1: 1–27. https://doi.org/10.1007/s11104-013-1630-3.

Enright, D. J., K. M. Frangioso, K. Isobe, D. M. Rizzo, and S. I. Glassman. 2022. "Mega-Fire in Redwood Tanoak Forest Reduces Bacterial and Fungal Richness and Selects for Pyrophilous Taxa That Are Phylogenetically Conserved." *Molecular Ecology* 31, no. 8: 2475–2493. https://doi.org/10.1111/mec.16399.

Fierer, N., J. A. Jackson, R. Vilgalys, and R. B. Jackson. 2005. "Assessment of Soil Microbial Community Structure by Use of Taxon-Specific Quantitative PCR Assays." *Applied and Environmental Microbiology* 71, no. 7: 4117–4120. https://doi.org/10.1128/AEM.71.7.4117-4120.2005.

Floudas, D., M. Binder, R. Riley, et al. 2012. "The Paleozoic Origin of Enzymatic Lignin Decomposition Reconstructed From 31 Fungal Genomes." *Science* 336, no. 6089: 1715–1719. https://doi.org/10.1126/science.1221748.

Fowler, A. F., B. Basso, N. Millar, and W. F. Brinton. 2023. "A Simple Soil Mass Correction for a More Accurate Determination of Soil Carbon Stock Changes." *Scientific Reports* 13, no. 1: 2242. https://doi.org/10.1038/s41598-023-29289-2.

Glassman, S. I., C. Weihe, J. Li, M. B. N. Albright, C. I. Looby, and A. C. Martiny. 2018. "Decomposition Responses to Climate Depend on Microbial Community Composition." *Proceedings of the National Academy of Sciences* 115, no. 47: 11994–11999. https://doi.org/10.1073/pnas.1811269115.

Graham, E. B., J. E. Knelman, A. Schindlbacher, et al. 2016. "Microbes as Engines of Ecosystem Function: When Does Community Structure Enhance Predictions of Ecosystem Processes?" *Frontiers in Microbiology* 7: 1–10. https://doi.org/10.3389/fmicb.2016.00214.

Hanes, T. L. 1971. "Succession After Fire in the Chaparral of Southern California." *Ecological Monographs* 41, no. 1: 27–52. https://doi.org/10.2307/1942434.

Hartig, F., and L. Lohse. 2021. *Residual Diagnostics for Hierarchical (Multi-Level/Mixed) Regression Models [R Package DHARMa Version 0.4. 4]*. R Core Team. https://CRAN.R-project.org/package=DHARMa.

Hatten, J. A., D. Zabowski, A. Ogden, and W. Thies. 2008. "Soil Organic Matter in a Ponderosa Pine Forest With Varying Seasons and Intervals of Prescribed Burn." *Forest Ecology and Management* 255, no. 7: 2555–2565. https://doi.org/10.1016/j.foreco.2008.01.016.

Högberg, M. N., and P. Högberg. 2002. "Extramatrical Ectomycorrhizal Mycelium Contributes One-Third of Microbial Biomass and Produces, Together With Associated Roots, Half the Dissolved Organic Carbon in a Forest Soil." *New Phytologist* 154, no. 3: 791–795. https://doi.org/10.1046/j.1469-8137.2002.00417.x.

Högberg, M. N., U. Skyllberg, P. Högberg, and H. Knicker. 2020. "Does Ectomycorrhiza Have a Universal Key Role in the Formation of Soil Organic Matter in Boreal Forests?" *Soil Biology & Biochemistry* 140: 107635. https://doi.org/10.1016/j.soilbio.2019.107635.

Horton, T. R., T. D. Bruns, and V. Thomas Parker. 2011. "Ectomycorrhizal Fungi Associated With Arctostaphylos Contribute to *Pseudotsuga menziesii* Establishment." *Canadian Journal of Botany. Journal Canadien de Botanique* 77: 93–102. https://doi.org/10.1139/b98-208.

Huang, W., W. Yu, B. Yi, et al. 2022. "Contrasting Geochemical and Fungal Controls on Decomposition of Lignin and Soil Carbon at Continental Scale." *Nature Communications* 14: 2227. https://doi.org/10.21203/rs.3.rs-2086399/v1.

Jilling, A., M. Keiluweit, A. R. Contosta, et al. 2018. "Minerals in the Rhizosphere: Overlooked Mediators of Soil Nitrogen Availability to Plants and Microbes." *Biogeochemistry* 139, no. 2: 103–122. https://doi.org/10.1007/s10533-018-0459-5.

Klink, S., A. B. Keller, A. J. Wild, et al. 2022. "Stable Isotopes Reveal That Fungal Residues Contribute More to Mineral-Associated Organic Matter Pools Than Plant Residues." *Soil Biology & Biochemistry* 168: 108634. https://doi.org/10.1016/j.soilbio.2022.108634.

Kurth, V. J., M. D. MacKenzie, and T. H. DeLuca. 2006. "Estimating Charcoal Content in Forest Mineral Soils." *Geoderma* 137, no. 1: 135–139. https://doi.org/10.1016/j.geoderma.2006.08.003.

Kuznetsova, A., P. B. Brockhoff, and R. H. B. Christensen. 2017. "lmerTest Package: Tests in Linear Mixed Effects Models." *Journal of Statistical Software* 82, no. 13: 1–26. https://doi.org/10.18637/jss.v082.i13.

Lavallee, J. M., J. L. Soong, and M. F. Cotrufo. 2020. "Conceptualizing Soil Organic Matter Into Particulate and Mineral-Associated Forms to Address Global Change in the 21st Century." *Global Change Biology* 26, no. 1: 261–273. https://doi.org/10.1111/gcb.14859.

Liang, C., J. P. Schimel, and J. D. Jastrow. 2017. "The Importance of Anabolism in Microbial Control Over Soil Carbon Storage." *Nature Microbiology* 2, no. 8: 1–6.

Licata, C., and R. Sanford. 2012. "Charcoal and Total Carbon in Soils From Foothills Shrublands to Subalpine Forests in the Colorado Front Range." *Forests, Trees and Livelihoods* 3, no. 4: 944–958. https://doi.org/10.3390/f3040944.

Liu, C. M., S. Kachur, M. G. Dwan, et al. 2012. "FungiQuant: A Broad-Coverage Fungal Quantitative Real-Time PCR Assay." *BMC Microbiology* 12: 255. https://doi.org/10.1186/1471-2180-12-255.

Maestre, F. T., B. M. Benito, M. Berdugo, et al. 2021. "Biogeography of Global Drylands." *New Phytologist* 231, no. 2: 540–558. https://doi.org/10.1111/nph.17395.

Maestrini, B., and J. R. Miesel. 2017. "Modification of the Weak Nitric Acid Digestion Method for the Quantification of Black Carbon in Organic Matrices." *Organic Geochemistry* 103: 136–139. https://doi.org/10.1016/j.orggeochem.2016.10.010.

Martin, M. 2011. "Cutadapt Removes Adapter Sequences From High-Throughput Sequencing Reads." *EMBnet.journal* 17, no. 1: 10–12. https://doi.org/10.14806/ej.17.1.200.

Marx, M.-C., M. Wood, and S. C. Jarvis. 2001. "A Microplate Fluorimetric Assay for the Study of Enzyme Diversity in Soils." *Soil Biology & Biochemistry* 33, no. 12: 1633–1640. https://doi.org/10.1016/S0038-0717(01)00079-7.

McLaren, J. R., K. M. Buckeridge, M. J. van de Weg, G. R. Shaver, J. P. Schimel, and L. Gough. 2017. "Shrub Encroachment in Arctic Tundra: *Betula nana* Effects on Above- and Belowground Litter Decomposition." *Ecology* 98, no. 5: 1361–1376. https://doi.org/10.1002/ecy.1790.

Merino, A., F. García-Oliva, M. T. Fontúrbel, and J. A. Vega. 2021. "The High Content of Mineral-Free Organic Matter in Soils Increases Their Vulnerability to Wildfire in Humid-Temperate Zones." *Geoderma* 395: 115043. https://doi.org/10.1016/j.geoderma.2021.115043.

Nelson, A. R., C. C. Rhoades, T. S. Fegel, et al. 2024. "Wildfire Impact on Soil Microbiome Life History Traits and Roles in Ecosystem Carbon Cycling." *ISME Communications* 4, no. 1: ycae108. https://doi.org/10.1093/ismeco/ycae108.

Nguyen, N. H., Z. Song, S. T. Bates, et al. 2016. "FUNGuild: An Open Annotation Tool for Parsing Fungal Community Datasets by Ecological Guild." *Fungal Ecology* 20: 241–248. https://doi.org/10.1016/j.funeco.2015.06.006.

Nicita, E., and E. Halverson. 2018. "Holy Fire Burned Area Emergency Response Soil Resource Report." https://www.fs.usda.gov/Internet/FSE_DOCUMENTS/fseprd594878.pdf.

Oksanen, J., F. G. Blanchet, R. Kindt, et al. 2013. "Package 'vegan.'" R Package Ver. 2.0–8, 254.

O'Leary, J. F. 1984. *Environmental Factors Influencing Postburn Vegetation in a Southern California Shrubland*. University of California.

Parsons, A., P. R. Robichaud, S. A. Lewis, C. Napper, and J. T. Clark. 2010. "Field Guide for Mapping Post-Fire Soil Burn Severity." USDA Forest Service, General Technical Report RMRS-GTR, 243, 1–49.

Pellegrini, A. F. A., A. C. Caprio, K. Georgiou, et al. 2021. "Low-Intensity Frequent Fires in Coniferous Forests Transform Soil Organic Matter in Ways That May Offset Ecosystem Carbon Losses." *Global Change Biology* 27: 3810–3823. https://doi.org/10.1111/gcb.15648.

Pellegrini, A. F. A., J. Harden, K. Georgiou, et al. 2021. "Fire Effects on the Persistence of Soil Organic Matter and Long-Term Carbon Storage." *Nature Geoscience* 15, no. 1: 5–13. https://doi.org/10.1038/s41561-021-00867-1.

Pellegrini, A. F. A., P. B. Reich, S. E. Hobbie, et al. 2023. "Soil Carbon Storage Capacity of Drylands Under Altered Fire Regimes." *Nature Climate Change* 13, no. 10: 1089–1094. https://doi.org/10.1038/s41558-023-01800-7.

Pérez-Valera, E., M. Verdú, J. A. Navarro-Cano, and M. Goberna. 2018. "Resilience to Fire of Phylogenetic Diversity Across Biological Domains." *Molecular Ecology* 27, no. 13: 2896–2908. https://doi.org/10.1111/mec.14729.

Pingree, M. R. A., P. S. Homann, B. Morrissette, and R. Darbyshire. 2012. "Long and Short-Term Effects of Fire on Soil Charcoal of a Conifer Forest in Southwest Oregon." *Forests, Trees and Livelihoods* 3, no. 2: 353–369. https://doi.org/10.3390/f3020353.

Plamboeck, A. H., T. E. Dawson, L. M. Egerton-Warburton, M. North, T. D. Bruns, and J. I. Querejeta. 2007. "Water Transfer via Ectomycorrhizal Fungal Hyphae to Conifer Seedlings." *Mycorrhiza* 17, no. 5: 439–447. https://doi.org/10.1007/s00572-007-0119-4.

Poeplau, C., A. Don, J. Six, et al. 2018. "Isolating Organic Carbon Fractions With Varying Turnover Rates in Temperate Agricultural Soils – A Comprehensive Method Comparison." *Soil Biology & Biochemistry* 125: 10–26. https://doi.org/10.1016/j.soilbio.2018.06.025.

Pressler, Y., J. C. Moore, and M. F. Cotrufo. 2019. "Belowground Community Responses to Fire: Meta-Analysis Reveals Contrasting Responses of Soil Microorganisms and Mesofauna." *Oikos* 128, no. 3: 309–327. https://doi.org/10.1111/oik.05738.

Pulido-Chavez, M. F., J. W. J. Randolph, C. Zalman, L. Larios, P. M. Homyak, and S. I. Glassman. 2022. "Rapid Bacterial and Fungal Successional Dynamics in First Year After Chaparral Wildfire." *Molecular Ecology* 32: 1685–1707. https://doi.org/10.1111/mec.16835.

Püspök, J. F., S. Zhao, A. D. Calma, et al. 2022. "Effects of Experimental Nitrogen Deposition on Soil Organic Carbon Storage in Southern California Drylands." *Global Change Biology* 29, no. 6: 1160–1679. https://doi.org/10.1111/gcb.16563.

R Core Team. 2023. "R: A Language and Environment for Statistical Computing (4.3.1)." https://www.R-project.org/.

RAWS USA Climate Archive. 2024. "Western Regional Climate Center." https://raws.dri.edu/.

Riley, K. L., and R. A. Loehman. 2016. "Mid-21st-Century Climate Changes Increase Predicted Fire Occurrence and Fire Season Length, Northern Rocky Mountains, United States." *Ecosphere* 7, no. 11: e01543. https://doi.org/10.1002/ecs2.1543.

Riley, R., A. A. Salamov, D. W. Brown, et al. 2014. "Extensive Sampling of Basidiomycete Genomes Demonstrates Inadequacy of the White-Rot/Brown-Rot Paradigm for Wood Decay Fungi." *Proceedings of the National Academy of Sciences of the United States of America* 111, no. 27: 9923–9928. https://doi.org/10.1073/pnas.1400592111.

Rocca, J. D., E. K. Hall, J. T. Lennon, et al. 2015. "Relationships Between Protein-Encoding Gene Abundance and Corresponding Process Are Commonly Assumed Yet Rarely Observed." *ISME Journal* 9, no. 8: 1693–1699. https://doi.org/10.1038/ismej.2014.252.

Rocci, K. S., J. M. Lavallee, C. E. Stewart, and M. F. Cotrufo. 2021. "Soil Organic Carbon Response to Global Environmental Change Depends on Its Distribution Between Mineral-Associated and Particulate Organic Matter: A Meta-Analysis." *Science of the Total Environment* 793: 148569. https://doi.org/10.1016/j.scitotenv.2021.148569.

Saiya-Cork, K. R., R. L. Sinsabaugh, and D. R. Zak. 2002. "The Effects of Long Term Nitrogen Deposition on Extracellular Enzyme Activity in an *Acer saccharum* Forest Soil." *Soil Biology & Biochemistry* 34, no. 9: 1309–1315. https://doi.org/10.1016/S0038-0717(02)00074-3.

Sanaei, A., A. Ali, and M. A. Z. Chahouki. 2018. "The Positive Relationships Between Plant Coverage, Species Richness, and Aboveground Biomass Are Ubiquitous Across Plant Growth Forms in Semi-Steppe Rangelands." *Journal of Environmental Management* 205: 308–318. https://doi.org/10.1016/j.jenvman.2017.09.079.

Schimel, J. P., and S. M. Schaeffer. 2012. "Microbial Control Over Carbon Cycling in Soil." *Frontiers in Microbiology* 3: 1–11. https://doi.org/10.3389/fmicb.2012.00348.

Schweigert, M., S. Herrmann, A. Miltner, T. Fester, and M. Kästner. 2015. "Fate of Ectomycorrhizal Fungal Biomass in a Soil Bioreactor System and Its Contribution to Soil Organic Matter Formation." *Soil Biology & Biochemistry* 88: 120–127. https://doi.org/10.1016/j.soilbio.2015.05.012.

Soil Survey Staff. 2024. "Natural Resources Conservation Service, United States Department of Agriculture. Official Soil Series Descriptions [WWW Document]." Web Soil Survey. https://websoilsurvey.nrcs.usda.gov/app/.

Stoof, C. R., J. G. Wesseling, and C. J. Ritsema. 2010. "Effects of Fire and Ash on Soil Water Retention." *Geoderma* 159, no. 3–4: 276–285. https://doi.org/10.1016/j.geoderma.2010.08.002.

Taylor, D. L., W. A. Walters, N. J. Lennon, et al. 2016. "Accurate Estimation of Fungal Diversity and Abundance Through Improved Lineage-Specific Primers Optimized for Illumina Amplicon Sequencing." *Applied and Environmental Microbiology* 82, no. 24: 7217–7226. https://doi.org/10.1128/AEM.02576-16.

Tredennick, A. T., G. Hooker, S. P. Ellner, and P. B. Adler. 2021. "A Practical Guide to Selecting Models for Exploration, Inference, and Prediction in Ecology." *Ecology* 102, no. 6: e03336. https://doi.org/10.1002/ecy.3336.

USDA, Forest Service, Missoula Fire Sciences Laboratory. 2018. "Fire Regimes of California Chaparral Communities: Information From the Pacific Southwest Research Station and LANDFIRE." In *Fire Effects Information System*. U.S. Department of Agriculture, Forest Service, Rocky Mountain Research Station, Missoula Fire Sciences Laboratory. Accessed December 17, 2024. www.fs.usda.gov/database/feis/fire_regimes/CA_chaparral/all.html.

VanderRoest, J. P., J. A. Fowler, C. C. Rhoades, et al. 2024. "Fire Impacts on the Soil Metabolome and Organic Matter Biodegradability." *Environmental Science & Technology* 58, no. 9: 4167–4180. https://doi.org/10.1021/acs.est.3c09797.

Vogl, R. J., and P. Schorr. 1972. "Fire and Manzanita Chaparral in the San Jacinto Mountains, California." *Ecology* 53, no. 6: 1179–1188. https://doi.org/10.2307/1935432.

von Haden, A. C., W. H. Yang, and E. H. DeLucia. 2020. "Soils' Dirty Little Secret: Depth-Based Comparisons Can Be Inadequate for Quantifying Changes in Soil Organic Carbon and Other Mineral Soil Properties." *Global Change Biology* 26, no. 7: 3759–3770. https://doi.org/10.1111/gcb.15124.

Walker, X. J., J. L. Baltzer, S. G. Cumming, et al. 2019. "Increasing Wildfires Threaten Historic Carbon Sink of Boreal Forest Soils." *Nature* 572, no. 7770: 520–523. https://doi.org/10.1038/s41586-019-1474-y.

Wang, C., T. Cheng, S. Tang, M. Li, D. Zhang, and X. Pan. 2023. "Protective-Mechanism-Exclusive Thermal Stability Modes of Soil Organic Matter: Novel Implication for Wildfire Effect on Soil Organic Carbon." *Science of the Total Environment* 861: 160734. https://doi.org/10.1016/j.scitotenv.2022.160734.

Wang, Q., M. Zhong, and S. Wang. 2012. "A Meta-Analysis on the Response of Microbial Biomass, Dissolved Organic Matter, Respiration, and N Mineralization in Mineral Soil to Fire in Forest Ecosystems." *Forest Ecology and Management* 271: 91–97. https://doi.org/10.1016/j.foreco.2012.02.006.

Wardle, D. A., G. Hörnberg, O. Zackrisson, M. Kalela-Brundin, and D. A. Coomes. 2003. "Long-Term Effects of Wildfire on Ecosystem Properties Across an Island Area Gradient." *Science* 300, no. 5621: 972–975. https://doi.org/10.1126/science.1082709.

Werth, M., and Y. Kuzyakov. 2010. "^{13}C Fractionation at the Root–Microorganisms–Soil Interface: A Review and Outlook for Partitioning Studies." *Soil Biology & Biochemistry* 42, no. 9: 1372–1384. https://doi.org/10.1016/j.soilbio.2010.04.009.

Whelan, J. A., N. B. Russell, and M. A. Whelan. 2003. "A Method for the Absolute Quantification of cDNA Using Real-Time PCR." *Journal of Immunological Methods* 278, no. 1–2: 261–269. https://doi.org/10.1016/s0022-1759(03)00223-0.

Whitman, T., E. Whitman, J. Woolet, M. D. Flannigan, D. K. Thompson, and M.-A. Parisien. 2019. "Soil Bacterial and Fungal Response to Wildfires in the Canadian Boreal Forest Across a Burn Severity Gradient." *Soil Biology & Biochemistry* 138: 107571. https://doi.org/10.1016/j.soilbio.2019.107571.

Whitman, T., J. Woolet, M. Sikora, D. B. Johnson, and E. Whitman. 2022. "Resilience in Soil Bacterial Communities of the Boreal Forest From One to Five Years After Wildfire Across a Severity Gradient." *Soil Biology & Biochemistry* 172: 108755. https://doi.org/10.1016/j.soilbio.2022.108755.

Yilmaz, P., L. W. Parfrey, P. Yarza, et al. 2014. "The SILVA and "All-Species Living Tree Project (LTP)" Taxonomic Frameworks." *Nucleic Acids Research* 42, no. D1: D643–D648. https://doi.org/10.1093/nar/gkt1209.

Supporting Information

Additional supporting information can be found online in the Supporting Information section. **Data S1:** gcb70404-sup-0001-Supinfo.docx.